Phosphorylation of the Scc2 cohesin deposition complex subunit regulates chromosome condensation through cohesin integrity

Julie Woodman[a,b], Matthew Hoffman[b], Monika Dzieciatkowska[b], Kirk C. Hansen[b], and Paul C. Megee[a,b]

[a]Molecular Biology Program and [b]Department of Biochemistry and Molecular Genetics, University of Colorado School of Medicine, Aurora, CO 80045

ABSTRACT **The cohesion of replicated sister chromatids promotes chromosome biorientation, gene regulation, DNA repair, and chromosome condensation. Cohesion is mediated by cohesin, which is deposited on chromosomes by a separate conserved loading complex composed of Scc2 and Scc4 in *Saccharomyces cerevisiae*. Although it is known to be required, the role of Scc2/Scc4 in cohesin deposition remains enigmatic. Scc2 is a phosphoprotein, although the functions of phosphorylation in deposition are unknown. We identified 11 phosphorylated residues in Scc2 by mass spectrometry. Mutants of *SCC2* with substitutions that mimic constitutive phosphorylation retain normal Scc2–Scc4 interactions and chromatin association but exhibit decreased viability, sensitivity to genotoxic agents, and decreased stability of the Mcd1 cohesin subunit in mitotic cells. Cohesin association on chromosome arms, but not pericentromeric regions, is reduced in the phosphomimetic mutants but remains above a key threshold, as cohesion is only modestly perturbed. However, these *scc2* phosphomimetic mutants exhibit dramatic chromosome condensation defects that are likely responsible for their high inviability. From these data, we conclude that normal Scc2 function requires modulation of its phosphorylation state and suggest that *scc2* phosphomimetic mutants cause an increased incidence of abortive cohesin deposition events that result in compromised cohesin complex integrity and Mcd1 turnover.**

Monitoring Editor
Kerry S. Bloom
University of North Carolina

Received: Mar 20, 2015
Revised: Aug 27, 2015
Accepted: Sep 4, 2015

INTRODUCTION

The evolutionarily conserved cohesin complex is essential for the maintenance of genome integrity. Cohesins tether replicated sister chromatids together in a process called cohesion, which ensures accurate chromosome segregation to daughter cells by promoting bipolar spindle microtubule attachments (Eckert *et al.*, 2007; Onn *et al.*, 2008). Cohesins also facilitate DNA double-strand break repair by homologous recombination and play multiple roles in the maintenance of chromosome architecture that promote chromosome condensation in mitosis and variable diversity joining (VDJ) recombination in immunoglobulin genes in interphase cells (Guacci *et al.*, 1997; Ünal *et al.*, 2004; Ribeiro de Almeida *et al.*, 2012). In addition, cohesins mediate long-range chromatin interactions that affect the transcriptional regulation of a subset of metazoan genes. Defects in this process result in human cohesinopathies such as Cornelia de Lange syndrome, a severe developmental disease affecting multiple organ systems (for review, see Liu and Krantz, 2009; Horsfield *et al.*, 2012). Thus understanding how many critical nuclear processes are faithfully executed will require a fuller understanding of cohesin regulation.

Cohesin complexes assemble through tripartite interactions involving a heterodimer of structural maintenance of chromosomes (SMC) proteins Smc1 and Smc3 and a kleisin subunit, known in budding yeast as Mcd1/Scc1 (Guacci *et al.*, 1997; Michaelis *et al.*, 1997; Losada *et al.*, 1998). SMCs are members of a family of ATP-binding cassette transporter-like chromosomal ATPases that mediate a

This article was published online ahead of print in MBoC in Press (http://www.molbiolcell.org/cgi/doi/10.1091/mbc.E15-03-0165) on September 9, 2015.

J.W. and P.C.M. designed the research and wrote the article. J.W., M.H., and M.D. performed the research. K.C.H. contributed analytical tools.

Address correspondence to: Paul C. Megee (Paul.Megee@UCDenver.edu).

Abbreviations used: ChIP, chromatin immunoprecipitation; rDNA, ribosomal DNA.

variety of chromosomal processes that include chromosome condensation and repair in addition to cohesion. Within the cohesin complex, Mcd1 binds to both SMC ATPase domains, promoting their interaction (Haering *et al.*, 2002; Arumugam *et al.*, 2003; Gruber *et al.*, 2003; Weitzer *et al.*, 2003). Of interest, Mcd1 stability is dependent on its association with both SMC subunits (Toth *et al.*, 1999). Mcd1 is also mediates the tripartite ring's association with the fourth cohesin subunit, Scc3/SA1, whose function in the complex remains obscure (Zhang *et al.*, 2013; Orgil *et al.*, 2015).

The establishment of cohesion requires cohesin deposition onto chromosomes by the evolutionarily conserved, heterodimeric Scc2/Scc4 complex in budding yeast (Ciosk *et al.*, 2000). Cohesins copurify with Scc2/Scc4, suggesting that Scc2/Scc4 directly mediates deposition (Toth *et al.*, 1999; Ciosk *et al.*, 2000; D'Ambrosio *et al.*, 2008). Scc2/Scc4 plays no role in cohesin assembly, however, as cohesin subunits accumulate and form rings normally in conditional *scc2-4* or *scc4-4* mutants (Ciosk *et al.*, 2000). Although Scc2 and Scc4 protein levels remain constant through the cell division cycle, the chromatin association of Scc2/Scc4 is biphasic, reaching its highest levels in post–S-phase cells (Kogut *et al.*, 2009; Woodman *et al.*, 2014), suggesting involvement of unknown regulatory mechanisms. In addition, the molecular function(s) of Scc2/Scc4 in deposition also remain enigmatic but may involve stimulating cohesin's ATPase activity, which is essential for deposition (Weitzer *et al.*, 2003). Alternatively, Scc2/Scc4 may facilitate conformational changes in cohesin structure that promote its loading, consistent with the in vitro finding that the fission yeast Scc2 orthologue makes contacts with all four cohesin subunits (Murayama and Uhlmann, 2014; Soh *et al.*, 2015).

Cohesin's postdeposition chromatin association is regulated by several cohesin-associated factors. Cohesin's initial chromatin association is inherently unstable due to an antiestablishment activity mediated by Wpl1/Wapl (Gerlich *et al.*, 2006; Bernard *et al.*, 2008; McNairn and Gerton, 2009; Chan *et al.*, 2012; Eichinger *et al.*, 2013; Ladurner *et al.*, 2014). However, Wpl1 activity is inhibited in part during S phase by the Eco1/Ctf7 acetyltransferase, whose modification of conserved Smc3 lysine residues stabilizes chromatin-associated cohesin complexes (Ivanov *et al.*, 2002; Rowland *et al.*, 2009). Wpl1 activity is also antagonized by Pds5, which associates with cohesin and promotes cohesion maintenance (Hartman *et al.*, 2000; Stead *et al.*, 2003). Of interest, reduced Mcd1 stability has been noted when either Wpl1 is deleted or Pds5 is inactivated (Chan *et al.*, 2012; Tong and Skibbens, 2014). Thus Mcd1 stability is critically dependent on its interactions with other cohesin subunits and with a number of cohesin-associated proteins. Whether Mcd1 contributes to additional cohesin regulatory mechanisms remains an important unanswered question.

Evidence suggests that Scc2/Scc4 continues to play important roles even after cohesion establishment in S phase. Recent studies indicate that Scc2 participates in gene regulation, noncoding RNA biogenesis, and translational fidelity (Zuin *et al.*, 2014; Zakari and Gerton, 2015; Zakari *et al.*, 2015). Furthermore, Scc2 inactivation in postreplicative cells, the period when Scc2/Scc4 achieves its maximal chromatin association levels, results in decreased cell viability (Furuya *et al.*, 1998; Woodman *et al.*, 2014). It has been suggested that Scc2/Scc4 is a general loader of SMC complexes, and, as such, its inactivation in post–S-phase cells would adversely affect chromosome condensation due to defective condensin loading. However, Scc2/Scc4–condensin interactions have not been detected (D'Ambrosio *et al.*, 2008), instead suggesting that post–S-phase cohesin deposition has critical roles in other aspects of mitotic chromosome structure, such as chromosome condensation.

That Scc2 and its orthologues are phosphorylated (Villén *et al.*, 2007; Dephoure *et al.*, 2008; Wilson-Grady *et al.*, 2008; Woodman *et al.*, 2014) suggests the intriguing possibility that Scc2/Scc4 activities in cohesin deposition are subject to phosphoregulation. We showed previously that dephosphorylation of whole-cell extract leaves phosphoprotein Scc2 susceptible to regulated amino-terminal proteolysis, which disrupts Scc2–Scc4 interactions, as well as the complex's cohesin deposition activity (Woodman *et al.*, 2014). This observation is consistent with a recent structural study of amino-terminal Scc2 residues 1–181 with Scc4, which concluded that unfolding or proteolysis is required for Scc2–Scc4 dissociation (Hinshaw *et al.*, 2015). To define more precisely the role of Scc2 phosphorylation in cohesin deposition, we mapped Scc2 phosphorylation sites and determined the cellular consequences of *scc2* mutations that either prevent phosphorylation or constitutively mimic its effects. Our data suggest that the cohesin complex is regulated, in part, through Mcd1 protein stability and that the phosphorylation state of Scc2 plays a critical role in maintaining necessary levels of Mcd1.

RESULTS

Scc2 is phosphorylated at multiple residues

To elucidate the function of Scc2 phosphorylation, we first mapped phosphorylation sites within Scc2 using phosphopeptide enrichment and mass spectrometry (MS; see *Materials and Methods*). Briefly, Scc2-hexahistidine (6His)-3FLAG (hereafter referred to as Scc2-FLAG) was immunopurified from yeast cells and subjected to in-gel trypsin digestion followed by immobilized metal affinity chromatography to enrich for phosphopeptides in preparation for MS. Scc2 tryptic peptides recovered in MS analyses represented 77% of the total protein sequence, which increased an additional 6% when semitryptic peptides were included, resulting in the identification of 61 candidate phosphorylation sites throughout Scc2, as summarized in Supplemental Table S1 (MS data have been deposited with the ProteomeXchange Consortium [Vizcaino *et al.*, 2014] via the PRIDE partner repository with the data set identifier PXD001830 and 10.6019/PXD001830). Stringent criteria appropriate for enriched protein samples, described in detail in *Materials and Methods*, were used to select phosphosites for further analysis (Supplemental Table S1). Of 11 residues that met these criteria, eight sites (T67, S127, S157, S163, T231, T236, S305, and S320, where T and S refer to threonine and serine, respectively) cluster within Scc2's amino terminus (Figure 1A). Of note, this region of Scc2 mediates its interaction with its binding partner, Scc4, and these interactions are essential for the chromatin association of the Scc2/Scc4 complex (Watrin *et al.*, 2006; Takahashi *et al.*, 2008; Bermudez *et al.*, 2012; Braunholz *et al.*, 2012; Woodman *et al.*, 2014). Internal (S753) and carboxyl-terminal (S1182, S1185) sites of phosphorylation that met the established criteria were also identified in Scc2 and are located within or adjacent to predicted Huntingtin, elongation factor 3, protein phosphatase 2A, and yeast kinase TOR1 (HEAT) repeat domains (Figure 1A), named for proteins that contain these motifs. Of interest, HEAT repeats have been shown to mediate protein interactions, as well as DNA binding (Neuwald and Hirano, 2000; Piazza *et al.*, 2014).

Scc2 phosphomimetic mutants exhibit decreased viability and sensitivity to genotoxic agents

To assess directly the effects of phosphorylation at these sites, we generated *scc2* mutants that either mimic or abolish phosphorylation by substituting serine/threonine residues with glutamate (E) or alanine (A), respectively. Residues were mutated in groups based on

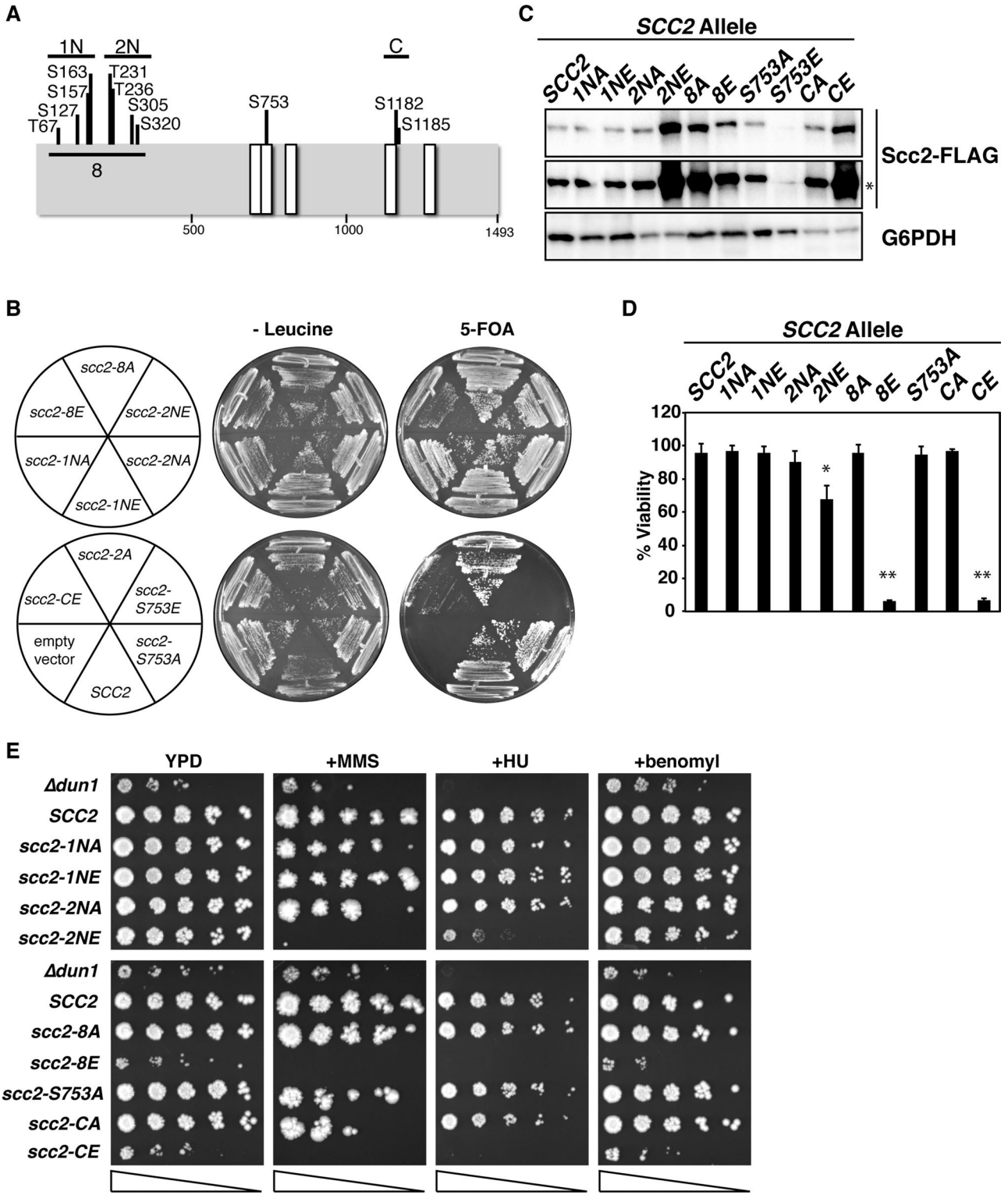

FIGURE 1: *scc2* phosphomimetic mutants have decreased viabilities and sensitivities to genotoxic agents. (A) Immobilized metal affinity chromatography and mass spectrometry were used to identify phosphorylated Scc2 residues, indicated by amino acid residue and number in a schematic of Scc2 (drawn approximately to scale), in extracts of Scc2-FLAG *cdc16-1* cells (1891-32C) arrested in mitosis at 37°C for 3 h. Vertical black lines indicate groupings of amino acids mutated simultaneously, labeled 1N, 2N, 8, and C, where N and C indicate amino- and carboxyl-terminal Scc2 residues, respectively, and 1, 2, and 8 indicate the first or second group of four amino terminal phosphoresidues, or all eight amino terminal phosphosites, respectively. Open boxes indicate the locations of HEAT repeat motifs, according to the UniProt database. (B) Isogenic *SCC2-FLAG* and *scc2-FLAG* phosphomutant strains (JWY179-JWY190) were inoculated on synthetic minimal medium lacking leucine or on complete synthetic medium containing 5-FOA. Plates were photographed after 3 d of growth at 23°C, except for the 5-FOA plate containing *scc2* carboxyl-terminal

their proximity to one another in the linear Scc2 protein sequence (Figure 1A). Accordingly, the eight amino- terminal phosphorylated residues (T67, S127, S157, S163, T231, T236, S305, and S320) were mutated simultaneously to glutamate or alanine residues, creating alleles *scc2-8E* and *scc2-8A*, respectively. In addition, the amino-terminal residues were mutated in two groups of four substitutions, denoted *scc2-1NA/E* and *scc2-2NA/E*, where 1N and 2N indicate the first four or second four phosphorylated residues in the amino (N)-terminal group of eight residues, respectively. Similarly, carboxyl (C)-terminal residues S1182 and S1185 were mutated together (*scc2-CA/E*), whereas S753 was analyzed as a single-substitution mutant.

Because Scc2 is an essential protein, we first determined whether mutations that constitutively alter the phosphorylation landscape of Scc2 affect cell viability. FLAG-tagged *SCC2* or *scc2* phosphomutant alleles under the control of the endogenous *SCC2* promoter were integrated ectopically at *LEU2* in a host strain containing a deletion of the endogenous *SCC2* locus and rescued with a *URA3* vector containing *SCC2*. Phosphomutants capable of supporting viability in the absence of wild-type *SCC2* were then identified by inoculating the cells on medium containing 5-fluoro-orotic acid (5-FOA; Boeke *et al.*, 1984), which kills cells that must retain the *SCC2*/*URA3* vector (Figure 1B). Although the *scc2-8E* and *scc2-CE* mutants grew slowly in the absence of plasmid-borne *SCC2*, only the *scc2*-S753E mutant failed to form colonies on 5-FOA. To determine whether these growth defects were caused by altered stability of the Scc2 phosphomutant proteins, we analyzed samples from all phosphomutant strains before 5-FOA exposure by immunoblot (Figure 1C). Whereas Scc2 protein levels were not reduced in any of the viable phosphomutants, they were noticeably reduced in the *scc2-S753E* mutant, with only trace amounts detectable upon overexposure. Taken together, these observations indicate that a mutation that mimics the constitutive phosphorylation of S753 causes inviability through protein instability. Whether this instability reflects an increased susceptibility of the mutant Scc2-S753E protein to amino-terminal cleavage is unknown. We note, however, that S753 is located within a HEAT repeat motif that is likely to play an integral role in Scc2 structure, suggesting that its mutation may alter protein folding, leading to its degradation by a pathway that is independent of amino-terminal cleavage.

The remaining nine viable *scc2* phosphomutants were further analyzed to determine whether altering Scc2 phosphorylation compromises Scc2 function, which include both S-phase and post–S-phase roles (Furuya *et al.*, 1998; Woodman *et al.*, 2014; Xu *et al.*, 2015). Of interest, both plating efficiency and serial dilution growth assays demonstrate that whereas the *scc2* alanine phosphomutants and the *scc2-1NE* phosphomimetic mutant grow indistinguishably from an isogenic wild-type control, the *scc2-8E* and *scc2-CE* phosphomimetic mutants have significant reductions in colony formation, indicating reduced cell viabilities (Figure 1, D and E, left). Moreover, these two phosphomimetic mutants, as well as *scc2-2NE*, exhibit extreme sensitivities to growth on medium containing low doses of methyl methanesulfonate (MMS) or hydroxyurea (HU; Figure 1E), which induce DNA damage or replication stress, respectively. The sensitivities of these mutants to the drugs were similar to, or perhaps even more pronounced than, those of a deletion mutant of *DUN1*, which encodes a checkpoint kinase required for DNA damaged–induced transcription of DNA repair genes (Zhou and Elledge, 1993). By contrast, none of the mutants is sensitive to the microtubule-depolymerizing agent benomyl (Figure 1E). These observations eliminate the possibility that a sensitivity to a cell cycle delay per se, such as that initiated in response to altered kinetochore–microtubule attachments, explains the sensitivity of *scc2* phosphomimetic mutants to genotoxic agents. Furthermore, Rnr3 protein levels are only weakly elevated in *scc2-8E* and *scc2-CE* mutants and are undetectable in *scc2-2NE* mutant cells (Supplemental Figure S1A). These observations argue strongly against the possibility that the DNA damage checkpoint is constitutively active in *scc2* phosphomimetic mutants, given that Rnr3 is a ribonucleotide reductase subunit that is strongly induced upon activation of the DNA damage checkpoint. Consistent with this conclusion, we find little evidence for substantial delays in cell cycle progression in phosphomutant cells when released synchronously from a G1 arrest (Supplemental Figure S1B). With the possible exception of *scc2-CE,* the *scc2* phosphomutants progressed through S phase normally and entered the next cell cycle indistinguishably from isogenic wild-type control cells. By contrast, *scc2-CE* phosphomimetic mutant cells appeared to delay slightly in G2/M, as indicated by the absence of cells in the population with 1C DNA contents at 150 min postrelease. Given that Scc2's role in cell cycle progression is largely unaffected in the mutants, it seems likely that altering the phosphorylation state of Scc2 through phosphomimetic mutation interferes with its ability to meet the increased demand for cohesin deposition required when cells are challenged with genotoxic agents (Ünal *et al.*, 2004; Heidinger-Pauli *et al.*, 2010).

scc2-8A mutant acquires novel Scc2 phosphorylation sites

A clear implication of the observed phenotypes of the *scc2* phosphomimetic mutants is that the ability to modulate the phosphorylation state of Scc2 is critical for its normal function. We therefore considered the possibility that the absence of phenotypes in the *scc2* alanine substitution mutants is due to compensatory phosphorylation of alternate sites in Scc2 in these mutants. To determine whether this possibility was indeed the case, we examined the phosphorylation state of Scc2-8A, in which eight amino-terminal S/T residues were made nonphosphorylatable by alanine substitution. Of interest, we found, using MS, that neighboring residues (S43, S74, S162, and T360) within the amino terminus of Scc2-8A were phosphorylated at sites not previously found to be modified in wild-type Scc2 (Supplemental Table S2). In addition, the carboxy terminus of Scc2-8A also had an altered phosphorylation profile. Whereas S1185 was clearly phosphorylated in Scc2-8A, there was a notable absence of S1182 phosphorylation, which had been found in eight

phosphomutants (bottom right), which was photographed after 5 d. (C) Immunoblots of wild-type and mutant Scc2-FLAG proteins, with a longer exposure indicated by an asterisk, and G6PDH from *scc2* phosphomutant cells before FOA shuffling (JWY179-JWY189). (D) The viabilities of *scc2* phosphomutant cells (JWY216-JWY225) obtained in plating efficiency experiments shown with SDs; $n = 3$. Student's *t* test determined the significance *p*; $*p < 0.03$, $**p < 0.0001$. (E) Isogenic *SCC2* and *scc2* phosphomutant cells (JWY216-JWY225 and Y03798) were grown to mid log phase, counted, subjected to fivefold serial dilutions, and then spotted onto plates containing rich medium without any drug (YPD) or rich medium containing 0.03% MMS, 50 mM HU, or 5 µg/ml benomyl. Triangles indicate decreasing cell densities from left to right. Plates were photographed after 3 d of growth.

independent MS analyses of wild-type Scc2. Instead, novel sites of phosphorylation, namely S1179 and S1183, were acquired in Scc2-8A. These data are consistent with the hypothesis that compensatory patterns of phosphorylation in the alanine substitution mutants may promote normal function of the Scc2 cohesin deposition complex subunit. In addition, these results suggest the interesting possibility that amino-terminal phosphorylation of Scc2 contributes to the regulation of the phosphorylation landscape of the entire protein.

scc2 phosphomutants interact with Scc4 and bind chromatin

In vitro treatment of whole-cell extract with phosphatase has been shown to promote amino- terminal cleavage of Scc2, leading to the loss of Scc2–Scc4 interactions (Woodman *et al.*, 2014). Such an approach is imprecise, however, due to its inability to target specific residues or groups of residues. Nevertheless, these observations suggest that the phosphorylation state of Scc2 may play a role in regulating Scc2–Scc4 interactions. To determine unambiguously the ability of the phosphomutants to affect this interaction, we subjected the *scc2* phosphomutants to reciprocal coimmunoprecipitation analyses. *SCC4*-6His-13Myc (hereafter referred to as Scc4-Myc) cells with integrated *SCC2*-FLAG or *scc2* phosphomutants were presynchronized in G1 using αF and then released into a G2/M arrest with nocodazole, at which point reciprocal coimmunoprecipitations were performed and analyzed via immunoblot (Figure 2). Overall no obvious changes in Scc2–Scc4 interactions were observed in the *scc2* phosphomutants when compared with an isogenic wild-type control, indicating that the altered phosphorylation states of the Scc2 residues tested do not affect Scc2–Scc4 interactions. In addition, these data suggest that compromised Scc2–Scc4 interactions are unlikely to be responsible for the drug sensitivities and reduced cell viabilities observed in *scc2* phosphomimetic mutants.

We next asked whether the chromatin association of Scc2/Scc4 is altered in the *scc2* phosphomimetic mutants, using chromatin immunoprecipitation (ChIP). Cells first presynchronized with α–factor (αF) mating pheromone were released to a mitotic arrest in media containing nocodazole and then processed for ChIP. We found that the levels of pericentromeric and arm cohesin-associated regions (CARs) present in Scc2 ChIPs were similar in *scc2* phosphomimetic (Figure 3A) and alanine (Figure 3B) substitution mutants and were indistinguishable from those in isogenic wild-type control cells, or even slightly increased in the case of the *scc2-2NE* mutant. These observations indicate that the chromatin association of Scc2/Scc4 is not reduced by changes in the phosphorylation states of Scc2 that were tested.

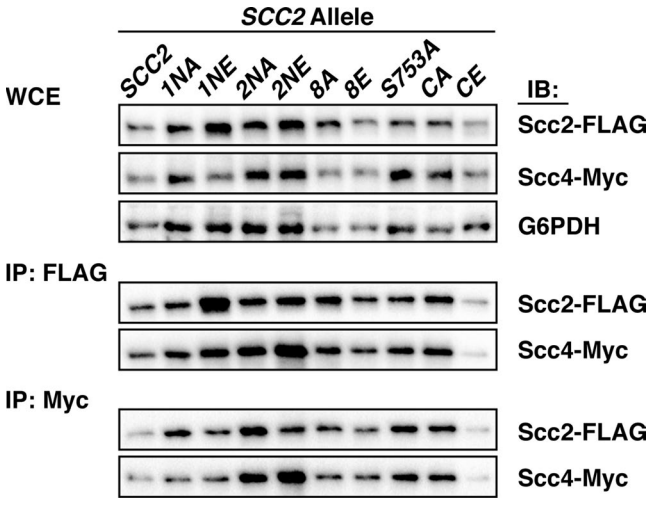

FIGURE 2: Scc2–Scc4 interactions are unaffected in *scc2* phosphomutants. Scc4-MYC cells expressing the indicated FLAG-tagged *SCC2* alleles (JWY216-JWY225) were first arrested in mitosis with nocodazole, and then precleared whole-cell extracts were immunoprecipitated with either FLAG- or MYC-bound magnetic protein A beads. Immunoblots of the levels of Scc2-FLAG and Scc4-MYC in input (WCE) and immunoprecipitation samples.

Cohesin binding to chromosome arms is modestly reduced in *scc2* phosphomimetic mutants

Our observations eliminate defects in either Scc2–Scc4 interactions or Scc2 chromatin association as potential reasons for the poor viabilities observed in the *scc2* phosphomimetic mutants. Thus we next determined whether the poor viabilities correlate with defects in sister chromatin cohesion, by monitoring the tethering of sister chromatids. To do this, we first integrated *SCC2* or *scc2* phosphomutants ectopically at *LEU2* in a host strain in which the endogenous *SCC2* gene was fused to an auxin-inducible domain (AID) that promotes proteasome-mediated proteolysis of AID-tagged proteins after the addition of a plant auxin, indole-3 acetic acid (IAA), to the culture medium (*Materials and Methods*). These cells also contained the Lac repressor protein (LacI) fused to green fluorescent protein (GFP) and tandem Lac operators integrated at *LYS4* on the arm of chromosome IV (Eng *et al.*, 2014). Cells were staged in G1 with αF, and Scc2-AID degradation was induced in G1 by the addition of IAA to the culture medium for 1 h. Cells were then scored for the presence of one or two GFP spots after release from G1 and arrest in G2/M in media containing nocodazole and IAA. If sister chromatid cohesion is maintained under these conditions, only one GFP spot is detected, whereas two GFP spots indicate precocious sister chromatid separation. We found that cells dependent solely on *scc2* phosphomimetic mutants for Scc2 function exhibited a twofold increase in separated sister chromatids relative to isogenic wild-type cells ($p < 0.05$). These defects are mild, however, when compared with empty vector control cells lacking any form of Scc2 (~18 vs. ~80% of cells with two GFP spots, respectively; Figure 4A).

We then performed ChIP of the Mcd1 cohesin subunit in cells in which the *scc2* phosphomutants were the sole source of Scc2 function to determine whether specific regions of chromosomes are particularly susceptible to reduced cohesin association levels after changes in the phosphorylation state of Scc2. Cells were then processed for ChIP as described. No significant differences in Mcd1 chromatin association were observed in any of the *scc2* alanine phosphomutants compared with those of an isogenic *SCC2* strain (Figure 4B). Similarly, the levels of pericentromeric sequences present in Mcd1 ChIPs were indistinguishable in *scc2* phosphomimetic and wild-type *SCC2* cells (Figure 4C, top). However, the levels of sequences corresponding to two different chromosome arm CAR sites on CHRs XII and III, were reduced approximately twofold in the Mcd1 ChIPs of the *scc2* phosphomimetic mutants compared with an isogenic wild-type control (Figure 4C, middle and bottom), consistent with the modest precocious separation defects we observed microscopically using a chromosome arm reporter location. Reduced Mcd1 chromatin association levels in the *scc2* phosphomimetic mutants cannot be attributed to altered cohesin–Scc2/Scc4 associations, however, as we found that Mcd1 coimmunoprecipitates with Scc2 in mitotically arrested *scc2* phosphomutants at levels that are indistinguishable from those of the isogenic wild-type Scc2 control

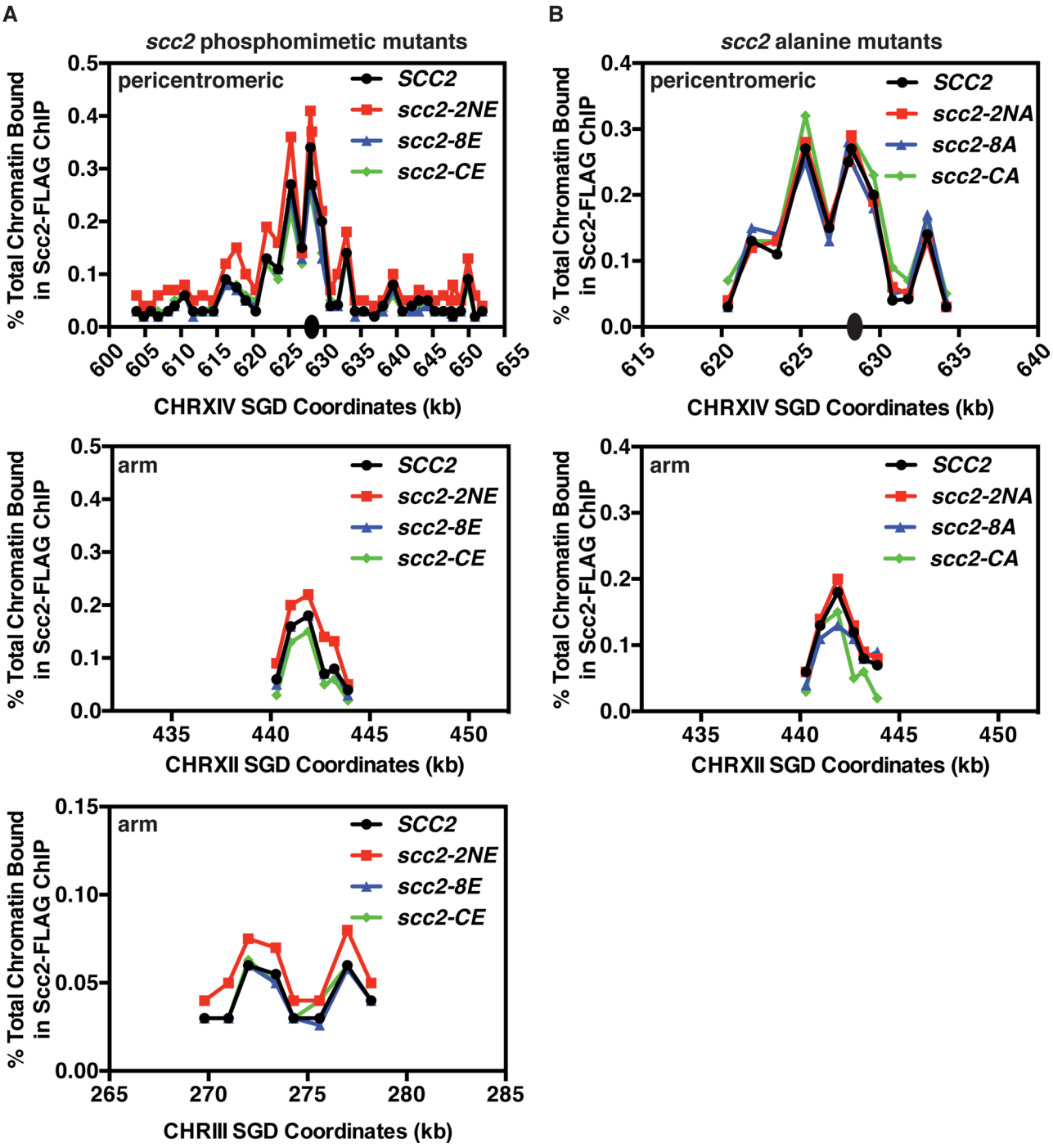

FIGURE 3: Scc2 chromatin association is not reduced in *scc2* phosphomutants. Isogenic *SCC2*-3FLAG (JWY216) and *scc2* phosphomutant cells (JWY217-JWY225) were arrested in mitosis with nocodazole for 3 h and processed for ChIP using anti-FLAG antibody. Scc2-FLAG distributions are shown in *scc2* phosphomimetic (A) and alanine substitution mutants (B) within CHRXIV pericentromeric regions (top) and CHRXII (middle) and CHRIII (A, bottom) arm sites, respectively. The position of the CHRXIV centromere is indicated by a black oval. Quantitation of DNA in the ChIPs, expressed as the percentage of the input DNA, is plotted as a function of the locations of the midpoints of the DNA fragments based on *Saccharomyces cerevisiae* Genome Database (SGD) coordinates. ChIPs were performed at least twice, and representative data from one biological replicate are shown.

(Supplemental Figure S2). Thus these results indicate that cohesin association is modestly compromised along chromosome arms in *scc2* phosphomimetic mutants even though Scc2/Scc4 remains present on chromatin and associates with cohesin at wild-type levels in these mutants.

scc2 phosphomimetic mutants have defects in chromosome condensation

Although it was reproducible, the rather mild cohesion defect in the *scc2* phosphomimetic mutants suggested that their high inviability is due to a defect in another chromosomal process. Given the

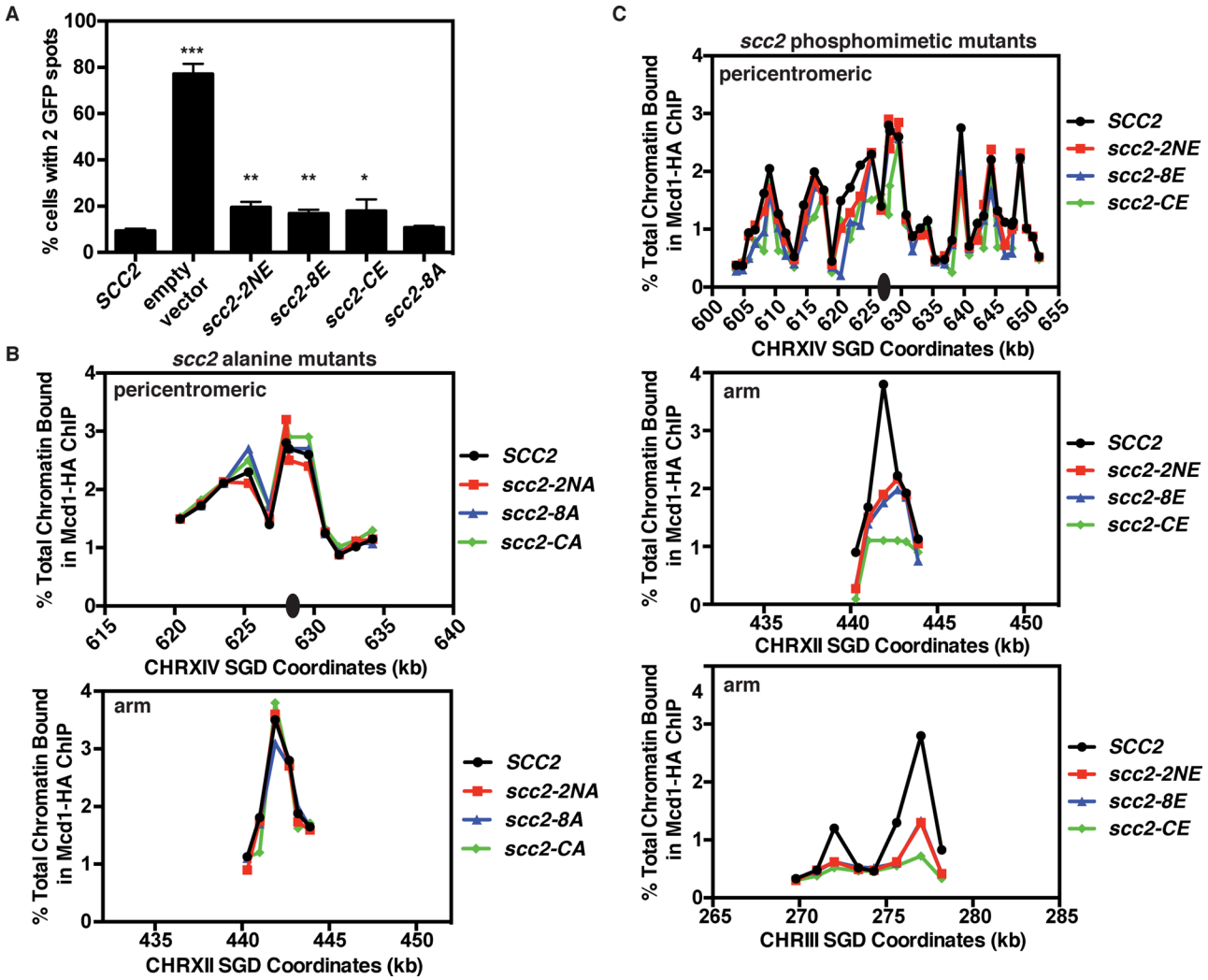

FIGURE 4: Mcd1 chromatin association is reduced along chromosome arms but not at pericentromeric regions. (A) Isogenic Scc2-AID cells with *SCC2-3FLAG* (JWY226), no ectopic *SCC2* allele (JWY254), or the indicated *scc2* phosphomimetic mutants integrated at *LEU2* (JWY230, JWY232, JWY236, and JWY231) were arrested in G1 with αF. IAA was added to induce turnover of wild-type Scc2-AID, and cells were released into medium containing IAA and nocodazole to arrest in mitosis. Cells were fixed in paraformaldehyde, and the number of GFP spots/nucleus was counted in 200 cells from each strain. Error bars represent SD; $n = 3$. Student's *t* test was performed to determine significance *p*; $*p < 0.05$, $**p < 0.002$, $***p < 0.0001$. (B, C) Mcd1-6HA cells containing the indicated *SCC2* (JWY216) or *scc2* phosphomutant alleles (JWY219, JWY221, JWY224), or *scc2* phosphomimetic alleles (JWY220, JWY222, and JWY225) were arrested in mitosis with nocodazole and processed for ChIP using anti-HA antibody to determine the levels of pericentromeric (CHRXIV [B, C, top]) and chromosome arm (B, bottom; C, middle and bottom) sequences present in Mcd1-HA ChIPs. Quantitation of DNA in ChIPs, expressed as a percentage of input DNA, is plotted as a function of the midpoints of the DNA fragments based on SGD coordinates. ChIPs were performed at least twice, and representative data from one biological replicate are shown. Black oval indicates the relative position of the centromere.

established role of cohesins in chromosome condensation (Guacci *et al.*, 1997; Lavoie *et al.*, 2002, 2004) and a strong correlation between condensation defects and cellular inviability (Guacci and Koshland, 2012; Orgil *et al.*, 2015), we monitored ribosomal DNA (rDNA) morphologies in wild-type and *scc2* phosphomutant cells. In G1-staged yeast, the CHRXII rDNA repeat has an amorphous appearance, protruding from the nuclear DNA mass. However, upon entry into mitosis, the rDNA repeat locus becomes highly organized and morphologically distinct, condensing into a continuous, line-like structure that can be visualized unambiguously as a "loop" emanating from the main DNA mass (Figure 5A). As previously demonstrated, the rDNA repeat in conditional *mcd1-1* or *scc2-4* mutant cells incubated at the restrictive temperature in mitosis becomes disorganized, reminiscent of the structure observed in G1 cells, rather than the continuous loop-like structure characteristic of mitotic cells (Guacci *et al.*, 1997; D'Ambrosio *et al.*, 2008; Figure 5A). To elucidate the role of Scc2 phosphorylation in chromosome condensation, we arrested isogenic *SCC2* and *scc2* phosphomutant cells lacking mitochondrial DNA in mitosis with nocodazole and fixed and processed them for rDNA visualization to analyze DNA and rDNA morphologies microscopically in the absence of potentially complicating mitochondrial DNA fluorescence (*Materials and Methods*). Of interest, ~90% of isogenic wild-type and *scc2* alanine substitution mutants exhibited morphologically normal rDNA loop formation, whereas ≥85% of mitotically arrested *scc2* phosphomimetic mutants exhibit amorphous rDNA structures with discontinuous, punctate

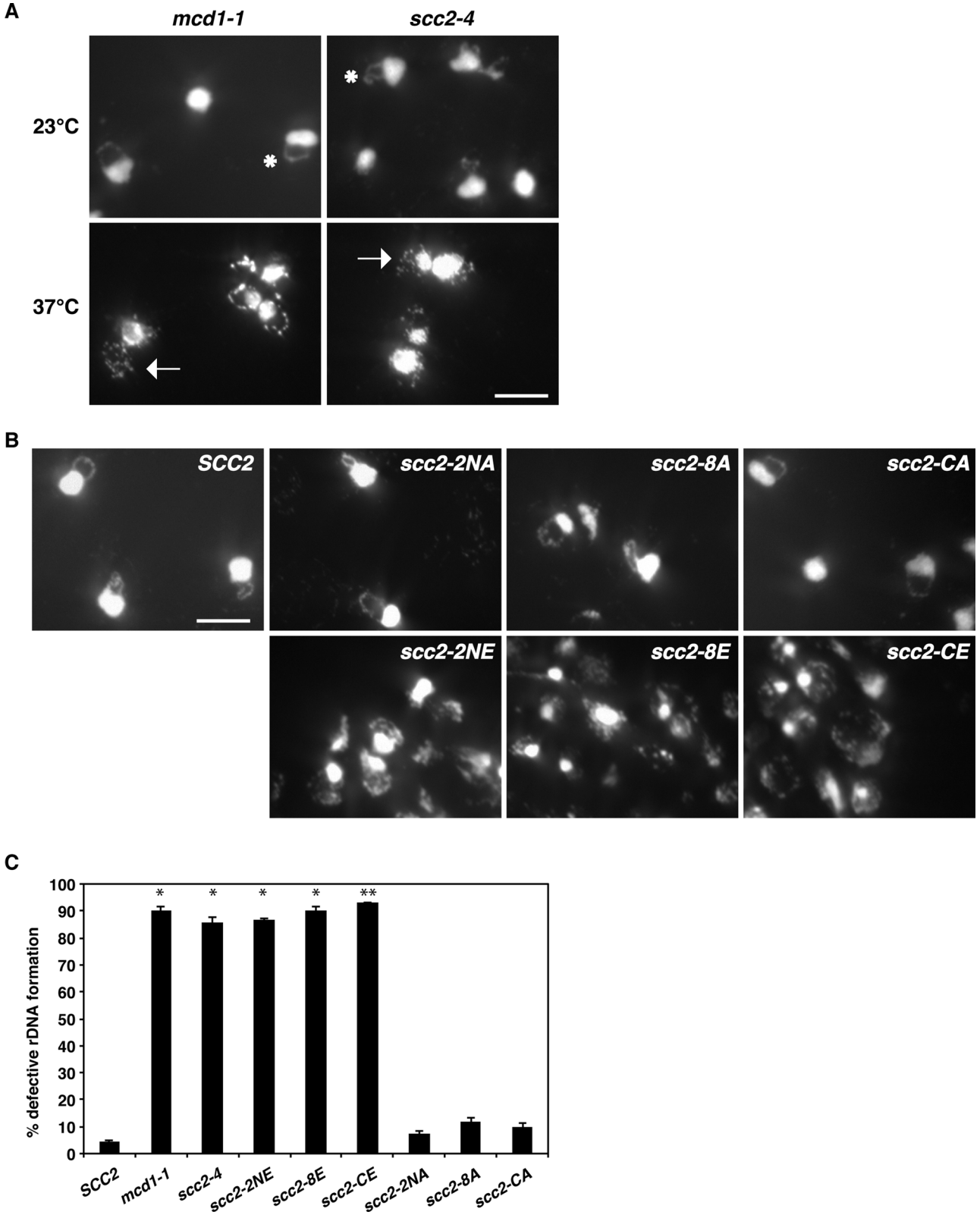

FIGURE 5: Condensation defects are prevalent in *scc2* phosphomimetic mutants. (A) *mcd1-1* and *scc2-4* cells (1813-4D and 2551-11D, respectively) were first arrested in mitosis using nocodazole at 23°C and either maintained at 23°C or shifted to 37°C for 1 h and then fixed and prepared for rDNA visualization as described in *Materials and Methods*. Asterisks indicate rDNA loops with continuous, line-like loop structures at 23°C, and arrows indicate amorphous, punctate structures at 37°C. White bar, 5 μm. (B) Isogenic *SCC2* and *scc2* phosphomutant strains lacking mitochondrial DNA (JWY247-JWY253) were arrested in mitosis using nocodazole and processed for rDNA visualization as described. White bar, 5 μm. (C) Percentage of "normal" vs. "defective" rDNA structures. For each experimental condition, 100 cells were scored with SDs; $n = 2$. Student's t test determined the significance p; $^{*}p < 0.01$, $^{**}p < 0.0001$.

foci, frequencies similar to those observed after Mcd1 or Scc2 inactivation in the corresponding conditional mutants (Figure 5, B and C). These observations indicate that, in addition to sensitivity to growth in the presence of genotoxic agents (Figure 1E) and mildly reduced cohesin binding along chromosome arms (Figure 4), the *scc2* phosphomimetic mutants have pervasive rDNA condensation defects. In addition, we note that while the *scc2-2NE* phosphomimetic mutant does indeed exhibit abnormal rDNA structures, this mutant retained more of the normal line-like, albeit punctate, rDNA structure as well as better cell viability than did the two other phosphomimetic mutants (Figure 1, D and E), again indicating the reduced viabilities of the *scc2* phosphomimetic mutants are strongly correlated with abnormal rDNA structure.

Mcd1 levels are reduced in *scc2* phosphomimetic mutants

Reduced cohesin association in arm, but not pericentromeric, CARs and chromosome condensation defects were observed previously when Mcd1 cohesin subunit levels were systematically lowered, suggesting that Mcd1 protein levels may also be reduced in the *scc2* phosphomimetic mutants (Heidinger-Pauli *et al.*, 2010). To determine whether this possibility is indeed the case, we monitored Mcd1 levels in isogenic *SCC2* or *scc2* phosphomimetic mutants after Scc2-AID degradation before S phase. Cell cultures were staged in G1 using αF and then split, with one-half receiving IAA for 1 h to induce Scc2-AID degradation and the other half being treated with dimethyl sulfoxide (DMSO) alone. Cells were then released from G1 into fresh medium containing either IAA or DMSO alone as before and allowed to progress synchronously through the cell cycle. Samples were taken at 30-min intervals for protein analysis upon release from G1 arrest, until cells had just reached G2/M. However, Mcd1 levels were maintained under these conditions in the *scc2* phosphomimetic mutants even in absence of Scc2-AID (Supplemental Figure S3A).

Given the dramatic defects in chromosome condensation, a late cell cycle event, in the *scc2* phosphomimetic mutants, we next determined whether Mcd1 stability is more vulnerable in mitotically arrested cells. The same strains described earlier were presynchronized in G1 and then released into a mitotic arrest with nocodazole, at which point Scc2-AID degradation was induced by IAA addition for 1 h. Samples for protein analyses were taken upon IAA addition and every 30 min thereafter. Of interest, while Mcd1 protein levels were only insignificantly reduced ($p = 0.23$) in cells lacking any Scc2 and were maintained, if not increased, in cells with integrated wild-type *SCC2*, Mcd1 levels were reduced approximately fourfold in phosphomimetic (*scc2-2NE, scc2-8E,* and *scc2-CE*) mutant mitotic cells treated with IAA for 90 min (Figure 6A). Although it is unclear why Mcd1 instability is specifically detected in postreplicative cells, one possibility is that Mcd1 instability increases in this cell cycle period due to the presence of higher levels of chromatin-associated Scc2/Scc4 (Woodman *et al.*, 2014), whose dysfunction in *scc2* phosphomimetic mutants appears to destabilize Mcd1. Moreover, that Mcd1 levels remain unaffected after Scc2-AID depletion in isogenic control cells lacking any other source of Scc2 suggests that Mcd1 destabilization in the *scc2* phosphomimetic mutants requires the physical interaction of the mutant Scc2 proteins with cohesin. This data suggest not only that Scc2 plays a critical role in maintaining Mcd1 levels through mitosis, but also that constitutive phosphorylation of Scc2 specifically disrupts this regulatory process.

Mcd1 instability is independent of Esp1 and Eco1

Mcd1 is normally degraded by the Esp1/separase protease at the metaphase/anaphase transition, thereby triggering sister chromatid

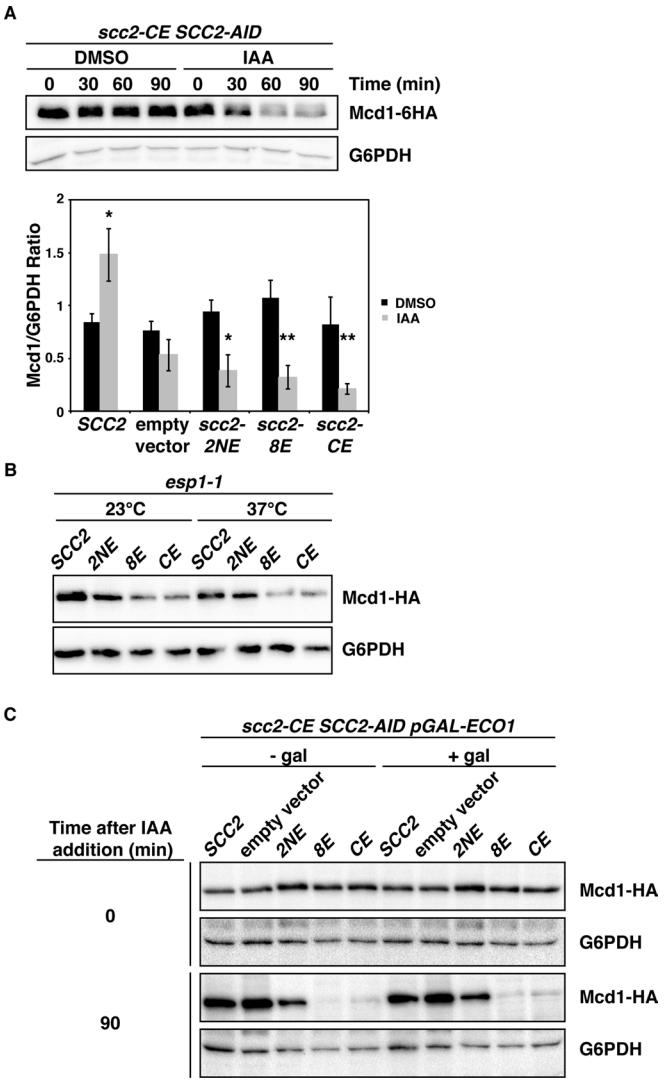

FIGURE 6: Mitotic Mcd1 protein levels are reduced in *scc2* phosphomimetic mutants. (A) Mcd1-HA Scc2-AID cells (JWY226, JWY230, JWY232, and JWY236) containing *SCC2*, no *SCC2* allele, or *scc2* phosphomimetic mutants integrated at *LEU2* (*scc2-2NE*, *scc2-8E*, *scc2-CE*) were arrested in mitosis with nocodazole, and Scc2-AID turnover was induced by IAA addition. Samples were prepared for protein analysis upon IAA addition (time 0) and every 30 min thereafter. Representative immunoblot of Mcd1 levels in *scc2-CE* mutant cells with and without IAA treatment. Quantitation of immunoblots of Mcd1-HA protein levels relative to G6PDH at 90 min after IAA addition normalized to Mcd1-HA/G6PDH at 0 min is shown with error bars indicating SD; $n = 3$. Student's *t* test determined the significance *p*; $*p < 0.05$ and $**p < 0.01$. (B) Isogenic *esp1-1* mutant cultures containing *SCC2* or *scc2* phosphomimetic mutants (JWY239-JWY242) were first arrested in mitosis with nocodazole and then split and incubated for 1 h at either 23 or 37°C. Immunoblots of Mcd1-HA and G6PDH. (C) *scc2* phosphomimetic mutant cells (JWY243-JWY246) carrying a plasmid that expresses *ECO1/CTF7* under the control of a galactose-inducible promoter were grown in noninducing/nonrepressing medium. Cell cultures were presynchronized in G1, released to a mitotic arrest in nocodazole, and split in half, and one-half was treated with galactose (2% final) for 1 h. All cultures were then treated with IAA, and protein samples were taken at the time of IAA treatment and every 30 min thereafter. The immunoblots show protein levels of Mcd1-HA and G6PDH at the time of IAA addition (time 0) and at 90 min of treatment.

separation (Uhlmann *et al.*, 1999). To rule out the possibility that the reduction in Mcd1 levels in mitotically arrested *scc2* phosphomimetic mutant cells is due to the premature activation of separase, we determined whether Mcd1 instability in these cells is Esp1 dependent. As a control, Mcd1 levels in isogenic *ESP1* and *esp1-1* mutant cells were first analyzed at 23 and 37°C to confirm that Mcd1 stability is unchanged after Esp1 inactivation in mitotically arrested cells (Supplemental Figure S3B). Conditional *esp1-1* mutant cells expressing various *scc2* phosphomutant alleles as the sole source of Scc2 were then arrested in mitosis with nocodazole, at which time the cultures were split and incubated at permissive or restrictive temperatures (23 or 37°C, respectively). We observed no change in Mcd1 levels by immunoblot after Esp1 inactivation (Figure 6B), suggesting that the Mcd1 instability observed in *scc2* phosphomimetic mutants is not due to premature activation of Esp1.

To test whether stabilizing cohesin complexes on chromatin is sufficient to rescue Mcd1 levels in the *scc2* phosphomutants, we determined the effect of Eco1/Ctf7 overexpression in the *scc2* phosphomutants. Eco1 normally acetylates Smc3 to promote the establishment of sister chromatid cohesion only during S phase, but Eco1 also becomes active outside of S phase when DNA damage is incurred. Moreover, induced Eco1 expression bypasses a requirement for DNA damage to produce "cohesive" cohesin chromatin association in G2/M cells (Ünal *et al.*, 2007). As before, Scc2-AID cells with *SCC2* or *scc2* phosphomutants integrated at *LEU2* that also express *ECO1* under the control of a galactose-inducible *GAL1* promoter on a *URA3* vector were grown in medium that allows rapid transcription of *GAL1*-regulated genes upon addition of galactose to the culture medium. Cells presynchronized in G1 using αF were released into a mitotic arrest using nocodazole. Once arrested, cultures were split in half, and galactose was added to one of the cultures for 1 h to induce Eco1 overexpression. IAA was then added to all cultures to induce the degradation of Scc2-AID, and aliquots of cells were taken upon IAA addition and every 30 min thereafter to monitor Mcd1 protein levels by immunoblot. Growth of control cells on galactose-containing medium produces functional Eco1, as indicated by complementation of a conditional *eco1/ctf7* mutant grown at the restrictive temperature (Supplemental Figure S3C). However, we found that the reduction in mitotic Mcd1 protein levels in *scc2* phosphomimetic mutant cells after Scc2-AID degradation was not reversed by Eco1 overexpression (Figure 6C). Of interest, as observed previously, Mcd1 stability was maintained in cells that lacked any source of Scc2 after IAA treatment, strongly suggesting that the Mcd1 instability observed in the *scc2* phosphomimetic cells occurs through an active engagement of cohesin with Scc2 phosphomimetic proteins that is apparently adversely affected by changes in Scc2 phosphorylation state. Collectively these data suggest that whereas Scc2 phosphorylation clearly affects Mcd1 protein stability, it does so independently of Esp1 or Eco1.

DISCUSSION

Although large-scale proteomics studies and a more recent biochemical study demonstrate that budding yeast Scc2 and its orthologues are phosphorylated, the consequences of this posttranslational modification on Scc2 function were not addressed previously (Villén *et al.*, 2007; Dephoure *et al.*, 2008; Wilson-Grady *et al.*, 2008; Woodman *et al.*, 2014). We find that although *scc2* mutations that prevent phosphorylation resulted in no obvious phenotypes, possibly due to the use of alternative phosphorylation sites throughout the protein, *scc2* phosphomimetic mutants exhibit sensitivity to genotoxic agents, substantial cellular inviability, and decreased cellular Mcd1 levels, demonstrating the importance of Scc2 phosphoregulation. Of importance, these *scc2* phosphomimetic mutants also have extensive defects in rDNA condensation but only mild sister chromatid cohesion defects. We infer from the rather modest arm cohesion defects in the *scc2* phosphomimetic mutants, as well as the existence of a cohesin-independent chromosome segregation mechanism in budding yeast (Guacci and Koshland, 2012), that the high levels of inviability in the *scc2* phosphomimetic mutants are not due to defects in sister chromatid cohesion. Instead, it seems more likely that this inviability is caused by the chromosome condensation defects we describe in these mutants. This conclusion is supported by the fact that both cellular inviability and a severe condensation defect present in an *mcd1* ROCC (regulation of cohesion and condensation) domain mutant are suppressed by deletion of *WPL1*, whereas the mutant's cohesion defect is exacerbated despite the maintenance of normal chromosomal cohesin association levels, suggesting that the recovered viability in the double mutant is due to the restoration of chromosome condensation (Eng *et al.*, 2014). Moreover, it was recently shown that mutants in the stromalin conserved domain of the Scc3 cohesin subunit that have a high incidence of inviability exhibit severe chromosome condensation defects but only minor cohesin association defects, again suggesting that defective condensation in the cohesin mutants is responsible for cellular inviability (Orgil *et al.*, 2015). Finally, we note that chromosome condensation defects are frequently, but not always, associated with mutants that lower Mcd1/cohesin levels on chromosomes, specifically in cases in which Mcd1 levels were reduced either through genetic manipulation or through polysumoylation-associated degradation of Mcd1 in *pds5* mutants (Hartman *et al.*, 2000; Heidinger-Pauli *et al.*, 2010; D'Ambrosio and Lavoie, 2014; Tong and Skibbens, 2014).

We also note that the condensation defects in the *scc2* phosphomimetic mutants do not support a priori the proposal that rather than being a dedicated cohesin deposition factor, Scc2/Scc4 may instead be a general loader of SMC-containing complexes. This suggestion was derived from the appearance of rDNA condensation defects in conditional *scc2-4* mutants in budding yeast, as well as the colocalization on chromosomes of Scc2/Scc4 with condensin, an essential SMC-containing complex that mediates chromosome condensation (D'Ambrosio *et al.*, 2008; Dowen *et al.*, 2013). Several observations challenge this model, however. First, although cohesin is readily coimmunoprecipitated with Scc2/Scc4, condensin is not (D'Ambrosio *et al.*, 2008). Furthermore, condensin's chromosomal association is only partially reduced in *scc2-4* mutants (Ciosk *et al.*, 2000; D'Ambrosio *et al.*, 2008). Instead, the findings that cohesins promote proper condensin function during chromosome condensation and that condensin recruitment to chromosomes is independent of cohesins (Guacci *et al.*, 1997; Lavoie *et al.*, 2002) together suggest that condensation defects in the *scc2-4* mutant, and indeed the *scc2* phosphomimetic mutants, arise due to aberrant cohesin levels rather than a failure to load condensins. In fact, our results suggest that continuous cohesin loading may be required for condensation maintenance, perhaps directing condensin activity.

Our observations also confirm and extend previous findings regarding the existence of a hierarchical association of cohesins along chromosomes and further suggest that the execution of various chromosomal processes requires different in vivo concentrations of cohesins (Heidinger-Pauli *et al.*, 2010). Although the levels of cohesin association in the *scc2* phosphomimetic mutants are apparently below a threshold required for chromosome condensation, they are above the threshold required for normal pericentromeric cohesion. A mechanism that enriches Scc2/Scc4 recruitment within pericentromeric chromatin likely ensures that sufficient levels of functional

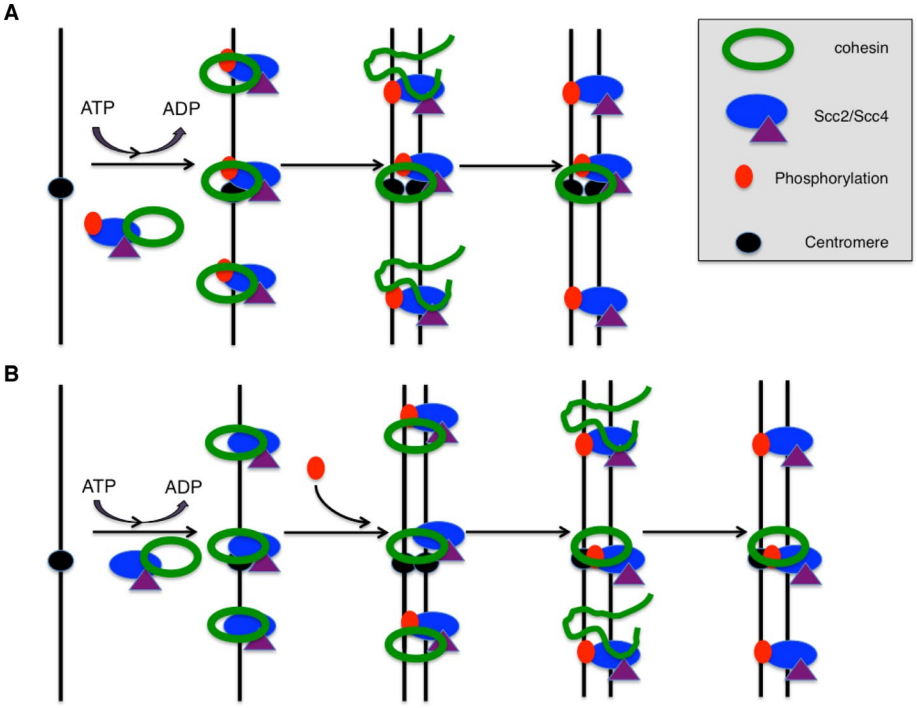

FIGURE 7: Constitutive Scc2 phosphorylation compromises mitotic cohesin integrity. Two models depicting ATP-dependent cohesin deposition. (A) Scc2/Scc4, phosphorylated at the time of its chromatin association, deposits cohesin rings onto chromosomes, depicted with black lines. Constitutive Scc2 phosphorylation during cohesin deposition increases the incidence of abortive cohesin-loading events, resulting in compromised cohesin integrity (unstructured green lines), which leads to Mcd1 instability along the entire length of the chromosome. Of note, reduced cohesin chromatin association is most dramatically observed along chromosome arms because the centromere-mediated enrichment of Scc2/Scc4 increases the frequency of successful pericentromeric loading events. (B) Chromosome arm–localized Scc2 is preferentially targeted for phosphorylation by an unknown mechanism after cohesin deposition. Scc2 phosphorylation actively promotes a conformation change in cohesin that compromises its integrity.

cohesins are maintained in these regions to promote chromosome biorientation (Eckert *et al.*, 2007; Kogut *et al.*, 2009; Natsume *et al.*, 2013), even in the *scc2* phosphomimetic mutants. By contrast, the reduced levels of arm cohesin association indicate that arm-associated cohesin is more sensitive to Scc2 phosphorylation, suggesting that cohesin association at arm CARs may be particularly amenable to remodeling by targeted Scc2 phosphorylation.

The phosphomimetic mutants described here represent a novel class of separation of function alleles of *SCC2* that enable rather robust levels of sister chromatid cohesion, especially within pericentromeric regions, but fail to promote proper chromosome condensation. By contrast, the only other (conditional) *scc2* alleles that have been described, *scc2-4* and *SCC2*-AID, cause severe defects in both sister chromatid cohesion establishment and chromosome condensation (D'Ambrosio *et al.*, 2008; Eng *et al.*, 2014). The dichotomy in phenotypes produced by *scc2* alleles may be related to differences in Mcd1 levels. Whereas cellular Mcd1 levels are significantly reduced in *scc2* phosphomimetic mutants, they are unaffected by Scc2 degradation in *SCC2*-AID cells lacking any other source of Scc2 (this study) or in *scc2-4* cells grown at a temperature that prevents cohesin deposition activity while having no effect on Scc2 stability (Ciosk *et al.*, 2000). We infer from these results, as well as our observation that Mcd1–Scc2 interactions are intact in *scc2* phosphomimetic mutants, that reduced Mcd1 levels result from compromised cohesin integrity in the *scc2* phosphomimetic mutants after the active engagement of mutant forms of Scc2 with cohesin (Figure 7), interactions that are eliminated after Scc2-AID degradation and at the restrictive temperature in the conditional *scc2-4* mutant.

Reductions in Mcd1 levels are not unique to *scc2* phosphomimetic mutants and also occur in mutants of other cohesin-associated factors, Wpl1 and Pds5. Mcd1 becomes extensively polysumoylated in conditional *pds5-1* mutants, leading to its proteasome-mediated degradation (D'Ambrosio and Lavoie, 2014; Tong and Skibbens, 2014). Similarly, deletion of *WPL1* also leads to reductions in cellular Mcd1 levels (Chan *et al.*, 2012). Of interest, Scc2, Wpl1, and Pds5 all associate with Mcd1, either indirectly through interactions with the Scc3 cohesin subunit or, in the case of Scc2, directly through interactions with Mcd1 (Rowland *et al.*, 2009; Murayama and Uhlmann, 2014; Orgil *et al.*, 2015). Of this group of Mcd1 stability regulators, all contain multiple HEAT repeats, although further investigation is required to determine whether HEAT repeat domains are critical for the maintenance of Mcd1 stability. In any case, regulating Mcd1 stability appears to be a ubiquitous mechanism to control cohesin association with chromosomes.

On the basis of our data, we favor the idea that mutations that mimic constitutive Scc2 phosphorylation interfere with one or more key steps in the cohesin deposition process, which ultimately compromises cohesin structure in a way that adversely affects Mcd1 integrity. One possibility is that Scc2 phosphorylation promotes or stabilizes ATP hydrolysis–dependent conformational changes in cohesin subunit structure associated with cohesin deposition (Figure 7; Hopfner *et al.*, 2000; Gruber *et al.*, 2006; Hu *et al.*, 2011). In such a model, *scc2* phosphomimetic mutants may trap cohesin deposition intermediates that are normally resolved by Scc2 dephosphorylation. Alternatively, Scc2 dephosphorylation, along with Eco1 and Pds5, may promote the stabilization of cohesin's chromatin association. In the latter scenario, a requirement for Scc2/Scc4 function would potentially extend beyond the cohesin deposition event per se, consistent with observations in both budding and fission yeast indicating that Scc2 inactivation after DNA replication, the interval when cohesin deposition normally occurs, reduces cellular viability (Furuya *et al.*, 1998; Woodman *et al.*, 2014). In both models, we postulate that *scc2* phosphomimetic mutants cause an increased incidence of abortive cohesin deposition events, which compromise cohesin complex integrity, resulting in reduced Mcd1 levels. The reduction of Mcd1 levels may be more evident in mitotically arrested cells due to the higher levels of Scc2/Scc4 that normally associate with chromosome at this cell cycle stage (Woodman *et al.*, 2014). Moreover, the inability of ectopic Eco1/Ctf7 expression to stabilize Mcd1/cohesin integrity in *scc2* phosphomimetic mutants suggests that constitutive Scc2 phosphorylation reduces either the number of cohesin complexes or their suitability as substrates for acetylation, suggesting that key aspect(s) of the cohesin deposition cycle are regulated by Scc2 phosphorylation.

In summary, the ability to fine-tune cohesin function through Scc2 phosphorylation presents a previously unappreciated avenue for cohesin regulation. Evidence that Scc2 orthologues from metazoans are also phosphorylated indicates that Scc2 phosphoregulation of cohesin complex integrity may be a conserved mechanism to promote refined control of cohesin function. Given that the human Scc2 orthologue, NIPBL, is mutated in ~60% of patients with the multisystem developmental disorder referred to as Cornelia de Lange syndrome, it will be of clinical interest to determine whether these mutations play a role in altering the phosphorylation profile of NIPBL and how these changes in NIPBL phosphorylation state may affect the etiology of the syndrome.

MATERIALS AND METHODS

Fe–nitrilotriacetic acid phosphopeptide enrichment and identification

Scc2-6His-3FLAG was immunopurified from cells at the indicated cell cycle phases using FLAG-bound magnetic beads. Because Scc2 exhibits greater stability during mitosis (Woodman *et al.*, 2014), cells used for phosphopeptide enrichment/mass spectrometry were first arrested in mitosis at 37°C using a temperature-sensitive *cdc16* strain. Samples were prepared for MS as previously described (Woodman *et al.*, 2014). Mitotic samples were also prepared for phosphopeptide enrichment using immobilized metal affinity chromatography (catalogue number 88300; ThermoFisher Pierce, Grand Island, NY) using the manufacturer's instructions and supplied buffers. The dry phosphopeptides were resuspended in 200 µl of binding buffer (5% acetic acid) and incubated with Fe–nitrilotriacetic acid beads for 20 min at room temperature with end-over-end rotation. Two 100-µl washes with buffer A (0.1% acetic acid) were followed by two washes of 100 µl buffer B (0.1% acetic acid, 10% acetonitrile). Phosphopeptides bound to the magnetic beads were eluted three times with 50 µl of elution buffer (0.1 M ammonium bicarbonate), pooled, desalted using graphite spin columns (Pierce), and resuspended in 20 µl of 0.1% formic acid. A volume of 8 µl was analyzed for each liquid chromatography MS/MS analysis by higher-energy collisional dissociation– and collision-induced dissociation–type fragmentation. Phosphosites chosen for further analysis included those with ion scores ≥20 (five phosphorylation sites were ≥53), as well as those with lower ion scores that met additional criteria. Those criteria included common fragmentation profiles and high mass accuracy when comparing phosphorylated and nonphosphorylated forms of the same peptides. The peptides identified were manually validated using positive identification of y and b fragment ions. Mascot software algorithms indicated the likelihood that a particular residue within a fragment peptide was phosphorylated relative to neighboring phosphorylatable residues within the same peptide (percent probability; Supplemental Table S1). Mass spectrometry data were deposited with the ProteomeXchange Consortium (Vizcaino *et al.*, 2014) via the PRIDE partner repository with the data set identifier PXD001830 and 10.6019/PXD001830.

Yeast strain construction

SCC2, *SCC4*, and *MCD1* were epitope tagged as previously described (Kogut *et al.*, 2009). *SCC2* was deleted from its chromosomal location using standard molecular biology techniques, and viability was maintained with plasmid pPCM102 (*CEN/ARS/SCC2/URA3*; Woodman *et al.*, 2014). The genotypes of yeast strains used in this study are listed in Supplemental Table S3.

The *scc2* phosphomutants were constructed essentially as described (Gibson *et al.*, 2009) using double-digested pJW4 (Woodman *et al.*, 2014) and multiple overlapping 500–base pair double-stranded DNA fragments (Integrated DNA Technologies, Coralville, IA; sequences available upon request) that span the *SCC2* open reading frame. pJW4 contains *SCC2*-6His-3FLAG in YCplac22 (Gietz and Sugino, 1988). For amino-terminal mutants *scc2-1N(A/E)*, *scc2-2N(A/E)*, and *scc2-8(A/E)*, *Afe*I/*Bst*EII-digested pJW4 was ligated in a single-step isothermal reaction with three overlapping 500–base pair DNA fragments that contained the desired nucleotide substitutions. *Pme*I/*Bse*RI-digested pJW4 was used to substitute nucleotides encoding for S753, and *Msc*I/*Xho*I-digested pJW4 was used with DNA fragments to make *scc2-CA* and *scc2-CE*. The reassembled vectors were each confirmed by DNA sequencing. Integrating vectors containing each of the phosphomutants were generated by subcloning, using the same restriction enzymes indicated, into pMH066, a YIplac128 vector containing wild-type *SCC2*-6His-3FLAG on a *Nar*I/*Bam*HI fragment blunt end ligated into the unique *Sma*I site of YIplac128. Vectors were linearized by *Cla*I digestion and integrated at *LEU2* in strain JWY208, whose sole copy of *SCC2* resides on pPCM102, a CEN/ARS plasmid carrying the *URA3* locus as a selectable marker.

Yeast cell culture and synchronization

Unless otherwise indicated, cells were cultured in rich medium at 23°C. Where indicated, cultures were synchronized in G1 by addition of αF mating pheromone at final concentrations of 3 µM or 15 nM for *BAR1* or *bar1* strains, respectively, to the culture media for a period of time equivalent to the generation time of the strain (typically 2.5–3 h), and confirmed microscopically. Cells arrested in nocodazole (15 µg/ml) were first synchronized in αF and then released from G1 arrest by washing twice with medium containing 0.1 mg/ml protease from *Streptomyces griseus* (Sigma-Aldrich, St. Louis, MO) and returned to growth in protease-containing medium that also contained nocodazole for ~3 h. G2/M arrests were confirmed by scoring cellular morphologies microscopically (Weber *et al.*, 2004). Phosphomutant cells were plated on 8 mM 5-FOA to determine the ability of the *scc2* phosphomutants to provide Scc2 function in the absence of wild-type *SCC2*.

Sensitivity to genotoxic agents

To survey sensitivities of *scc2* phosphomutants cells to genotoxic agents, cells were cultured on plates contained 0.03% MMS to induce DNA damage, 50 mM HU to cause DNA replication stress during S phase, or 5 mg/ml benomyl to affect microtubule dynamics.

Scc2-AID turnover

IAA (Gold Biotechnology, St. Louis, MO) was added to culture medium at a final concentration of 0.5 mM in 1% DMSO for 1 h to induce Scc2-AID turnover (Eng *et al.*, 2014).

Plating efficiency measurements

Cell viabilities were determined by measuring plating efficiencies. Briefly, cell densities of cultures were first determined by hemocytomer counting. Serial dilutions of each culture were then made to enable plating of ~200 cells/plate on rich medium in triplicate. Colonies formed at 23°C after 3 d (or 7 d in the case of slowly growing strains) were counted, and plating efficiencies were then calculated as the percentage of colonies formed as a function of the original number of cells plated.

Coimmunoprecipitation

To immunoisolate Scc2, protein A magnetic beads (ThermoFisher Invitrogen, Grand Island, NY) prebound overnight at 4°C to FLAG (Sigma-Aldrich) or Myc (Millipore, Billerica, MA) antibodies at ratios of 2–5 µg of serum to 10 µl of a 50% bead suspension were then

incubated with whole-cell extracts at 4°C for 2 h and washed thoroughly six times with 10 min between washes in 50 mM (4-(2-hydroxyethyl)-1-piperazineethanesulfonic acid, 100 mM KCl, 2.5 mM $MgCl_2$, 10% glycerol, 0.1% Triton, 0.1% Tween, and 300 mM NaCl plus the following protease and phosphatase inhibitors: 1 mM benzamidine, 0.5 mM sodium metabisulfite, 2.7 mg/ml pepstatin A, 4 mg/ml leupeptin, 1 mM phenylmethanesulfonyl fluoride, 2 mM sodium orthovanadate, 10 mM NaF, and 10 mM β-glycerophosphate (Woodman *et al.*, 2014). Samples were then subjected to immunoblotting as described later.

Chromatin immunoprecipitation

ChIP experiments were performed as previously described (Kogut *et al.*, 2009) without modification and with at least two biological replicates. Cells processed for ChIP were presynchronized in G1 with αF and released into fresh medium containing nocodazole for G2/M arrest.

Protein isolation and Western blotting

Proteins were isolated for analysis by treatment with 10% tricholoroacetic acid or by spheroplasting and lysing of a whole-cell extract with 1 mg/ml Zymolyase and 0.25% Triton-X, with the protease and phosphatase inhibitors indicated previously.

Immunoblotting and quantitation

SDS polyacrylamide gels (6%) were used to distinguish full-length and cleaved Scc2 species. Proteins were transferred to polyvinylidene difluoride membrane at 100 V for 1 h. Primary and secondary antibody solutions contained 1% bovine serum albumin, 1% dry nonfat milk, and 0.1% Tween in phosphate-buffered saline. Mouse monoclonal FLAG (Sigma-Aldrich) and hemagglutinin (Roche, Indianapolis, IN) antibodies, rabbit glucose-6-phosphate dehydrogenase (G6PDH; Sigma-Aldrich), and mouse polyclonal Myc serum (Millipore) were used at 5000-, 5000-, 75,000-, and 750-fold dilutions, respectively. Goat anti-mouse and anti-rabbit horseradish peroxidase–conjugated secondary antibodies (Bio-Rad, Hercules, CA) were used at 1:2500 and 1:10,000, respectively. Quantitation was performed using the Bio-Rad ChemiDoc System and ImageLab software.

Chromosome condensation analyses

rDNA was visualized in situ as previously described (Guacci *et al.*, 1994). To remove potentially complicating fluorescence contributions from mitochondrial DNA, phosphomutant cells were first grown to saturation twice in 25 μg/ml ethidium bromide to evict mitochondrial DNA (Goldring *et al.*, 1970). Strains that lacked mitochondrial DNA were identified by their inability to use glycerol as the sole carbon source. Cells were arrested in G2/M with nocodazole and fixed with 3.6% formaldehyde at 23°C for 2 h with gentle shaking. Chromosomal DNA was stained with 50 ng/ml 4′,6-diamidino-2-phenylindole and visualized using a Nikon Eclipse E800 fluorescence microscope equipped with a Plan APO 100× oil objective and a CoolSNAP HQ charge-coupled device camera (Photometrics, Tucson, AZ). Only loops or amorphous spots clearly associated with an intact spherical nuclear mass were counted in the scoring of the rDNA repeat morphologies.

ACKNOWLEDGMENTS

We thank M. Huang, D. Koshland, and R. Skibbens for strains and reagents and V. Guacci, M. Huang, and A. Johnson for technical advice. This work was supported by National Institutes of Health Grants R01 GM066213 (to P.C.M.) and T-32 GM008730 (to J.W.) and by an academic scholarship endowed by Victor and Earleen Bolie to the Molecular Biology Program at the University of Colorado Anschutz Medical Campus (to J.W.). This work was also supported in part by Flow Cytometry Shared Resource of the University of Colorado Cancer Center Support Grant P30CA046934.

REFERENCES

Arumugam P, Gruber S, Tanaka K, Haering CH, Mechtler K, Nasmyth K (2003). ATP hydrolysis is required for cohesin's association with chromosomes. Curr Biol 13, 1941–1953.

Bermudez VP, Farina A, Higashi TL, Du F, Tappin I, Takahashi TS, Hurwitz J (2012). *In vitro* loading of human cohesin on DNA by the human Scc2-Scc4 loader complex. Proc Natl Acad Sci USA 109, 9366–9371.

Bernard P, Schmidt CK, Vaur S, Dheur S, Drogat J, Genier S, Ekwall K, Uhlmann F, Javerzat JP (2008). Cell-cycle regulation of cohesin stability along fission yeast chromosomes. EMBO J 27, 111–121.

Boeke JD, LaCroute F, Fink GR (1984). A positive selection for mutants lacking orotidine-5′-phosphate decarboxylase activity in yeast: 5-fluoro-orotic acid resistance. Mol Gen Genet 197, 345–346.

Braunholz D, Hullings M, Gil-Rodriguez MC, Fincher CT, Mallozzi MB, Loy E, Albrecht M, Kaur M, Limon J, Rampuria A, *et al.* (2012). Isolated NIBPL missense mutations that cause Cornelia de Lange syndrome alter MAU2 interaction. Eur J Hum Genet 20, 271–276.

Chan KL, Roig MB, Hu B, Beckouet F, Metson J, Nasmyth K (2012). Cohesin's DNA exit gate is distinct from its entrance gate and is regulated by acetylation. Cell 150, 961–974.

Ciosk R, Shirayama M, Shevchenko A, Tanaka T, Toth A, Nasmyth K (2000). Cohesin's binding to chromosomes depends on a separate complex consisting of Scc2 and Scc4 proteins. Mol Cell 5, 243–254.

D'Ambrosio C, Schmidt CK, Katou Y, Kelly G, Itoh T, Shirahige K, Uhlmann F (2008). Identification of cis-acting sites for condensin loading onto budding yeast chromosomes. Genes Dev 22, 2215–2227.

D'Ambrosio LM, Lavoie BD (2014). Pds5 prevents the polySUMO-dependent separation of sister chromatids. Curr Biol 24, 361–371.

Dephoure N, Zhou C, Villén J, Beausoleil SA, Bakalarski CE, Elledge SJ, Gygi SP (2008). A quantitative atlas of mitotic phosphorylation. Proc Natl Acad Sci USA 105, 10762–10767.

Dowen JM, Bilodeau S, Orlando DA, Hubner MR, Abraham BJ, Spector DL, Young RA (2013). Multiple structural maintenance of chromosome complexes at transcriptional regulatory elements. Stem Cell Rep 1, 371–378.

Eckert CA, Gravdahl DJ, Megee PC (2007). The enhancement of pericentromeric cohesin association by conserved kinetochore components promotes high-fidelity chromosome segregation and is sensitive to microtubule-based tension. Genes Dev 21, 278–291.

Eichinger CS, Kurze A, Oliveira RA, Nasmyth K (2013). Disengaging the Smc3/kleisin interface releases cohesin from *Drosophila* chromosomes during interphase and mitosis. EMBO J 32, 656–665.

Eng T, Guacci V, Koshland D (2014). ROCC, a conserved region in cohesin's Mcd1 subunit, is essential for the proper regulation of the maintenance of cohesion and establishment of condensation. Mol Biol Cell 25, 2351–2364.

Furuya K, Takahashi K, Yanagida M (1998). Faithful anaphase is ensured by Mis4, a sister chromatid cohesion molecule required in S phase and not destroyed in G1 phase. Genes Dev 12, 3408–3418.

Gerlich D, Koch B, Dupeux F, Peters JM, Ellenberg J (2006). Live-cell imaging reveals a stable cohesin-chromatin interaction after but not before DNA replication. Curr Biol 16, 1571–1578.

Gibson DG, Young L, Chuang RY, Venter JC, Hutchison CA 3rd, Smith HO (2009). Enzymatic assembly of DNA molecules up to several hundred kilobases. Nat Methods 6, 343–345.

Gietz RD, Sugino A (1988). New yeast-*Escherichia coli* shuttle vectors constructed with in vitro mutagenized yeast genes lacking six-base pair restriction sites. Gene 74, 527–534.

Goldring ES, Grossman LI, Krupnick D, Cryer DR, Marmur J (1970). The petite mutation in yeast. Loss of mitochondrial deoxyribonucleic acid during induction of petites with ethidium bromide. J Mol Biol 52, 323–335.

Gruber S, Arumugam P, Katou Y, Kuglitsch D, Helmhart W, Shirahige K, Nasmyth K (2006). Evidence that loading of cohesin onto chromosomes involves opening of its SMC hinge. Cell 127, 523–537.

Gruber S, Haering CH, Nasmyth K (2003). Chromosomal cohesin forms a ring. Cell 112, 765–777.

Guacci V, Hogan E, Koshland D (1994). Chromosome condensation and sister chromatid pairing in budding yeast. J Cell Biol 125, 517–530.
Guacci V, Koshland D (2012). Cohesin-independent segregation of sister chromatids in budding yeast. Mol Biol Cell 23, 729–739.
Guacci V, Koshland D, Strunnikov A (1997). A direct link between sister chromatid cohesion and chromosome condensation revealed through the analysis of *MCD1* in *S. cerevisiae*. Cell 91, 47–57.
Haering CH, Lowe J, Hochwagen A, Nasmyth K (2002). Molecular architecture of SMC proteins and the yeast cohesin complex. Mol Cell 9, 773–788.
Hartman T, Stead K, Koshland D, Guacci V (2000). Pds5p is an essential chromosomal protein required for both sister chromatid cohesion and condensation in *Saccharomyces cerevisiae*. J Cell Biol 151, 613–626.
Heidinger-Pauli JM, Mert O, Davenport C, Guacci V, Koshland D (2010). Systematic reduction of cohesin differentially affects chromosome segregation, condensation, and DNA repair. Curr Biol 20, 957–963.
Hinshaw SM, Makrantoni V, Kerr A, Marston AL, Harrison SC (2015). Structural evidence for Scc4-dependent localization of cohesin loading. eLife 4, e06057.
Hopfner KP, Karcher A, Shin DS, Craig L, Arthur LM, Carney JP, Tainer JA (2000). Structural biology of Rad50 ATPase: ATP-driven conformational control in DNA double-strand break repair and the ABC-ATPase superfamily. Cell 101, 789–800.
Horsfield JA, Print CG, Monnich M (2012). Diverse developmental disorders from the one ring: distinct molecular pathways underlie the cohesinopathies. Front Genet 3, 171.
Hu B, Itoh T, Mishra A, Katoh Y, Chan KL, Upcher W, Godlee C, Roig MB, Shirahige K, Nasmyth K (2011). ATP hydrolysis is required for relocating cohesin from sites occupied by its Scc2/4 loading complex. Curr Biol 21, 12–24.
Ivanov D, Schleiffer A, Eisenhaber F, Mechtler K, Haering CH, Nasmyth K (2002). Eco1 is a novel acetyltransferase that can acetylate proteins involved in cohesion. Curr Biol 12, 323–328.
Kogut I, Wang J, Guacci V, Mistry RK, Megee PC (2009). The Scc2/Scc4 cohesin loader determines the distribution of cohesin on budding yeast chromosomes. Genes Dev 23, 2345–2357.
Ladurner R, Bhaskara V, Huis in 't Veld PJ, Davidson IF, Kreidl E, Petzold G, Peters JM (2014). Cohesin's ATPase activity couples cohesin loading onto DNA with Smc3 acetylation. Curr Biol 24, 2228–2237.
Lavoie BD, Hogan E, Koshland D (2002). In vivo dissection of the chromosome condensation machinery: reversibility of condensation distinguishes contributions of condensin and cohesin. J Cell Biol 156, 805–815.
Lavoie BD, Hogan E, Koshland D (2004). *In vivo* requirements for rDNA chromosome condensation reveal two cell-cycle-regulated pathways for mitotic chromosome folding. Genes Dev 18, 76–87.
Liu J, Krantz ID (2009). Cornelia de Lange syndrome, cohesin, and beyond. Clin Genet 76, 303–314.
Losada A, Hirano M, Hirano T (1998). Identification of *Xenopus* SMC protein complexes required for sister chromatid cohesion. Genes Dev 12, 1986–1997.
McNairn AJ, Gerton JL (2009). Intersection of ChIP and FLIP, genomic methods to study the dynamics of the cohesin proteins. Chromosome Res 17, 155–163.
Michaelis C, Ciosk R, Nasmyth K (1997). Cohesins: chromosomal proteins that prevent premature separation of sister chromatids. Cell 91, 35–45.
Murayama Y, Uhlmann F (2014). Biochemical reconstitution of topological DNA binding by the cohesin ring. Nature 505, 367–371.
Natsume T, Muller CA, Katou Y, Retkute R, Gierlinski M, Araki H, Blow JJ, Shirahige K, Nieduszynski CA, Tanaka TU (2013). Kinetochores coordinate pericentromeric cohesion and early DNA replication by Cdc7-Dbf4 kinase recruitment. Mol Cell 50, 661–674.
Neuwald AF, Hirano T (2000). HEAT repeats associated with condensins, cohesins, and other complexes involved in chromosome-related functions. Genome Res 10, 1445–1452.
Onn I, Heidinger-Pauli JM, Guacci V, Unal E, Koshland DE (2008). Sister chromatid cohesion: a simple concept with a complex reality. Annu Rev Cell Dev Biol 24, 105–129.
Orgil O, Matityahu A, Eng T, Guacci V, Koshland D, Onn I (2015). A conserved domain in the Scc3 subunit of cohesin mediates the interaction with both Mcd1 and the cohesin loader complex. PLoS Genet 11, e1005036.
Piazza I, Rutkowska A, Ori A, Walczak M, Metz J, Pelechano V, Beck M, Haering CH (2014). Association of condensin with chromosomes depends on DNA binding by its HEAT-repeat subunits. Nat Struct Mol Biol 21, 560–568.
Ribeiro de Almeida C, Stadhouders R, Thongjuea S, Soler E, Hendriks RW (2012). DNA-binding factor CTCF and long-range gene interactions in V(D)J recombination and oncogene activation. Blood 119, 6209–6218.
Rowland BD, Roig MB, Nishino T, Kurze A, Uluocak P, Mishra A, Beckouët F, Underwood P, Metson J, Imre R, *et al.* (2009). Building sister chromatid cohesion: Smc3 acetylation counteracts an antiestablishment activity. Mol Cell 33, 763–774.
Soh YM, Burmann F, Shin HC, Oda T, Jin KS, Toseland CP, Kim C, Lee H, Kim SJ, Kong MS, *et al.* (2015). Molecular basis for SMC rod formation and its dissolution upon DNA binding. Mol Cell 57, 290–303.
Stead K, Aguilar C, Hartman T, Drexel M, Meluh P, Guacci V (2003). Pds5p regulates the maintenance of sister chromatid cohesion and is sumoylated to promote the dissolution of cohesion. J Cell Biol 163, 729–741.
Takahashi TS, Basu A, Bermudez V, Hurwitz J, Walter JC (2008). Cdc7-Drf1 kinase links chromosome cohesion to the initiation of DNA replication in *Xenopus* egg extracts. Genes Dev 22, 1894–1905.
Tong K, Skibbens RV (2014). Cohesin without cohesion: a novel role for Pds5 in *Saccharomyces cerevisiae*. PLoS One 9, e100470.
Toth A, Ciosk R, Uhlmann F, Galova M, Schleiffer A, Nasmyth K (1999). Yeast cohesin complex requires a conserved protein, Eco1p(Ctf7), to establish cohesion between sister chromatids during DNA replication. Genes Dev 13, 320–333.
Uhlmann F, Lottspeich F, Nasmyth K (1999). Sister-chromatid separation at anaphase onset is promoted by cleavage of the cohesin subunit Scc1. Nature 400, 37–42.
Ünal E, Arbel-Eden A, Sattler U, Shroff R, Lichten M, Haber JE, Koshland D (2004). DNA damage response pathway uses histone modification to assemble a double-strand break-specific cohesin domain. Mol Cell 16, 991–1002.
Ünal E, Heidinger-Pauli JM, Koshland D (2007). DNA double-strand breaks trigger genome-wide sister-chromatid cohesion through Eco1 (Ctf7). Science 317, 245–248.
Villén J, Beausoleil SA, Gerber SA, Gygi SP (2007). Large-scale phosphorylation analysis of mouse liver. Proc Natl Acad Sci USA 104, 1488–1493.
Vizcaino JA, Deutsch EW, Wang R, Csordas A, Reisinger F, Rios D, Dianes JA, Sun Z, Farrah T, Bandeira N, *et al.* (2014). ProteomeXchange provides globally coordinated proteomics data submission and dissemination. Nat Biotechnol 32, 223–226.
Watrin E, Schleiffer A, Tanaka K, Eisenhaber F, Nasmyth K, Peters JM (2006). Human Scc4 is required for cohesin binding to chromatin, sister-chromatid cohesion, and mitotic progression. Curr Biol 16, 863–874.
Weber SA, Gerton JL, Polancic JE, DeRisi JL, Koshland D, Megee PC (2004). The kinetochore is an enhancer of pericentric cohesin binding. PLoS Biol. 2, 1340–1353.
Weitzer S, Lehane C, Uhlmann F (2003). A model for ATP hydrolysis-dependent binding of cohesin to DNA. Curr Biol 13, 1930–1940.
Wilson-Grady JT, Villén J, Gygi SP (2008). Phosphoproteome analysis of fission yeast. J Proteome Res 7, 1088–1097.
Woodman J, Fara T, Dzieciatkowska M, Trejo M, Luong N, Hansen KC, Megee PC (2014). Cell cycle-specific cleavage of Scc2 regulates its cohesin deposition activity. Proc Natl Acad Sci USA 111, 7060–7065.
Xu B, Sowa N, Cardenas ME, Gerton JL (2015). l-leucine partially rescues translational and developmental defects associated with zebrafish models of Cornelia de Lange syndrome. Hum Mol Genet 24, 1540–1555.
Zakari M, Gerton JL (2015). The SMC loader Scc2 regulates gene expression. Cell Cycle 14, 943.
Zakari M, Trimble Ross R, Peak A, Blanchette M, Seidel C, Gerton JL (2015). The SMC loader Scc2 promotes ncRNA biogenesis and translational fidelity. PLoS Genet 11, e1005308.
Zhang N, Jiang Y, Mao Q, Demeler B, Tao YJ, Pati D (2013). Characterization of the interaction between the cohesin subunits Rad21 and SA1/2. PLoS One 8, e69458.
Zhou Z, Elledge SJ (1993). DUN1 encodes a protein kinase that controls the DNA damage response in yeast. Cell 75, 1119–1127.
Zuin J, Franke V, van Ijcken WF, van der Sloot A, Krantz ID, van der Reijden MI, Nakato R, Lenhard B, Wendt KS (2014). A cohesin-independent role for NIPBL at promoters provides insights in CdLS. PLoS Genet 10, e1004153.